Theor Chim Acta (1988) 74: 23-38

Theoretica Chimica Acta

Intramolecular energy transfer in water

George G. Hall and Hideharu Nobutoki

Division of Molecular Engineering, Kyoto University, Sakyo-ku, Kyoto 606, Japan

(Received May 18; revised December 3/Accepted December 8, 1987)

The evolution of the vibrational motion of a water molecule which has been excited locally is studied. An exact solution is obtained of a model Hamiltonian representing the non-harmonic behaviour of the molecule. Since this is obtained numerically it does not explain what is observed but it leads to a simplified model of the motion in which different aspects can be isolated and discussed. For many initial modes, especially those of higher energy, there is a large initial drop in the probability of finding the energy in the original local mode. This is due to dephasing. The factors involved in dephasing are discussed. A simple hypothesis is suggested which leads to a formula for this drop and this agrees substantially with the graphical evidence. The relation between the drop and the amplitude of the initial mode is also discussed.

Key words: Dephasing — Quantum beats — Intramolecular energy transfer

1. Introduction

The migration of vibrational energy within a molecule is becoming a subject of great interest now that infrared lasers have made it easy to input considerable energy into molecular vibrations and experimental methods of detecting the effects have been developed. A review of these results for some molecules has been given by Weitz and Flynn [1].

Earlier papers by Freed and Nitzan [2] and by Stannard and Gelbart [3] have discussed the general features of the evolution of the excitation. Several stages have been distinguished. The first is often called dephasing since the different modes of vibration start with identical phase but rapidly lose this after a few oscillations. The second is characterized by beats in the probability functions. The importance of quantum beats for radiative decay has been emphasized by

Ivanco et al. [4]. In the third, the steady leakage of energy into other higher energy modes begins to be observed as a general decay of probability of the lower levels. In calculating this decay, random influences become more important and statistical arguments predominate (e.g. Ramaswamy et al. [5]). This paper is concerned with the first stage and the transition to the second. The decay effects are ignored.

In their paper [3] Stannard and Gelbart distinguish sharply between the behaviour of small molecules and large molecules. Here we deal only with the lower states of small molecules. The density of states is then too sparse for arguments using the golden rule to be appropriate. The water molecule is used as an example throughout.

The numerical solution of the dynamical equations is outlined in Sect. 2 and an approximate solution which can be obtained analytically in Sect. 3. The form of the molecular Hamiltonian is discussed in Sect. 4 and the different types of graph of the probability of the initial state are described. An important distinction is that between the results for initial states which are non-degenerate and those which are degenerate. The behaviour typical of these is outlined in Sects. 5 and 6. The most interesting quantity for this paper is the rapid initial drop in probability due to dephasing. This is defined in two ways in Sect. 7 and the results compared. Although it has not been possible to relate them exactly, the connection of the drop with the density of states is discussed in Sect. 9 and with the amplitude of the initial state in Sect. 10.

2. The exact solution

The initial behaviour of a molecule immediately after excitation is complicated. We assume that all the energy is concentrated initially into one local mode of vibration and that this energy is small compared with the dissociation energy. Because of the coupling of modes this energy can then excite many other modes but these are all discrete modes below the dissociative continuum.

The initial state will be called $|I\rangle$ and will be a local mode, not an eigenstate. Atomic units will be used throughout the paper. The Hamiltonian operator H, in a basis of local modes which are taken as normal and orthogonal, is now divided into diagonal and off-diagonal parts

$$H = D + V \tag{1}$$

so that D_r is the energy of the mode $|r\rangle$. The time dependent Schrödinger equation for the evolution of $|I\rangle$ is

$$\dot{\psi} = i(D + V)\psi \tag{2}$$

with the initial condition $\psi(0) = |I\rangle$.

The exact solution of the equation within the finite basis is obtained by a direct numerical method. The first step requires finding all the eigenvalues of the matrix H and, in the second step, the initial state is expanded in terms of its eigenvectors.

If the eigenvalues are E_s, the (time independent) eigenfunctions ψ_s and the expansion coefficients for $|I\rangle$ in terms of ψ_s are c_{Is} then the wave function for the evolving $|I\rangle$ is

$$\psi = \sum_s c_{Is} \exp(itE_s)\psi_s, \; |I\rangle = \sum_s c_{Is}\psi_s, \tag{3}$$

and the probability of finding the molecule in $|I\rangle$ after t is

$$P(t) = |\langle I|\psi\rangle|^2 = \left|\sum_s |c_{Is}|^2 \exp(itE_s)\right|^2 \tag{4}$$

$$= \sum_s |c_{Is}|^4 + \sum_{s>u} 2|c_{Is}|^2|c_{Iu}|^2 \cos(z_s - z_u)t. \tag{5}$$

The first term in (5) is constant and determines $\langle P\rangle$, the average value of P while the second consists of beats with the exact transition energies as frequencies. With modern computers and using a sufficiently large number of local modes, this solution can be evaluated numerically for any required value of t. Unfortunately it does not explain the structure of P nor the magnitude of c_{Is} in a physical way so that other solutions are required to achieve understanding of the results.

3. The one-state model

To explain the evolution process in more physical terms, ψ will be expanded in the local modes, $|s\rangle$, rather than the eigenfunctions, since they show where the excitation is located, thus

$$\psi = \sum_s a_s(t)|s\rangle \tag{6}$$

and the equations for the $a_s(t)$ become

$$\dot{a}_s = iD_s a_s + i\sum_u V_{su}a_u, \tag{7}$$

with

$$a_s(0) = \delta_{sI}. \tag{8}$$

The one-state model which we use to explain the process now retains only those elements of V which connect directly with the initial state. These should be the most important terms for the early stages of its evolution. This simplification allows the equations to be solved analytically. To obtain the solution for the evolution of the initial state it is convenient to use the Laplace transform method to solve the differential equations. A_s is the Laplace transform of a_s and Eqs. (7) and (8) become:

$$pA_I - 1 = i\left(D_I A_I + \sum_r V_{Ir}A_r\right) \tag{9}$$

$$pA_r = i(D_r A_r + V_{rI}A_I), \tag{10}$$

where we take $r \neq I$ in all the equations in this section. Eq. 10 can be solved directly so that

$$A_r = iV_{rI}A_I/(p - iD_r) \tag{11}$$

$$A_I = 1/\left(p - iD_I + \sum_r V_{Ir}V_{rI}/(p - iD_r)\right). \tag{12}$$

The eigenvalues of the model Hamiltonian are the zeros $p = iz_r$ (z_r is real) of the denominator of A_I. These can be calculated iteratively. The roots satisfy

$$z = D_I + \sum_r V_{Ir}V_{rI}/(z - D_r) \tag{13}$$

and for the root near D_I, D_I can be used as the first approximation on the right of the equation. But for other roots the expression needs to be rearranged by isolating the sth term,

$$z = D_s + V_{Is}V_{sI}/(z - D_I) + (z - D_s)/(z - D_I)\sum_r V_{Ir}V_{rI}/(z - D_r). \tag{14}$$

This second form allows D_s to be the first approximation to the nearest root z. Note that there is one root near D_I and those above this have $z_r > D_r$ whereas those less than this have $z_r < D_r$. If the roots include no repeated roots then A_I can be expressed in simple partial fractions as

$$A_I = \sum_s c_s/(p - iz_s) \tag{15}$$

and the solution will be

$$a_I = \sum_s c_s \exp(iz_s t). \tag{16}$$

The coefficient c_s is defined by the limit

$$c_s = \lim_{p \to iz_s} (p - iz_s) \Big/ \left(p - iD_I + \sum_r V_{Ir}V_{rI}/(p - iD_r)\right).$$

Using L'Hospital's rule this gives

$$c_s = 1 \Big/ \left(1 + \sum_r V_{Ir}V_{rI}/(z_s - D_r)^2\right), \tag{17}$$

where s includes all the possible states but r excludes I. It is obvious from this that $1 \geq c_s \geq 0$. (A state for which $V_{Is} = 0$ is non-interacting and must be excluded from the expansions. Since it has $z_s = D_s$ it will introduce indeterminate terms into the equations.) It can be seen from c_s that when D_I is very different from the other D_r then z_I becomes close to D_I and c_I tends to 1. Since, because of the initial condition, $\sum_s c_s = 1$ the remaining c_s must be rather small. More generally it can be seen that the main effect of the evolution is to mix into I the interacting local states close to it in energy. The probability of finding the molecule in the state I is now

$$P(t) = |\langle I|\psi\rangle|^2 = |a_I(t)|^2. \tag{18}$$

Since a_I is a sum of exponentials its product with its conjugate will have constant terms and cosine terms which are the beats.

$$P = \sum_s c_s^2 + 2 \sum_{s>u} c_s c_u \cos(z_s - z_u)t. \tag{19}$$

By comparing this expression with (5) it can be seen that c_s is the approximation to $|c_{Is}|^2$.

The one-state model does not allow the degeneracies of the real equations for a symmetrical molecule to be resolved in a way that takes full account of symmetry. The water vibrations contain some exact degeneracies among the local modes due to its two identical bonds. In particular, when I is itself degenerate the model ignores terms in V of equal importance to those included. By using the symmetry fully we can extend the one-state model to make it rather more accurate.

In this modification the initial mode and some other modes will be assumed degenerate in pairs, e.g. $D_s = D_{s'}$. Such degeneracy can be resolved by taking + and − combinations of the modes. Thus we have symmetric modes, including + combinations of each pair together with the non-degenerate modes, and anti-symmetric modes which all have − combinations. This allows fully for a permutation symmetry between the local modes. The extension to more elaborate symmetries follows the same principles but requires a more deliberate use of group theory.

As a result of this transformation there are two Hamiltonian matrices which can be treated separately. The symmetric matrix has diagonal elements which are the energies of the symmetric combinations, i.e. $D_s + V_{ss'}$. The off-diagonal elements are $V_{Is} + V_{Is'}$, or $V_{Is}\sqrt{2}$ when s is non-degenerate. The restriction to the off-diagonal elements which connect with the initial mode is made after the transformation. This means that more than twice as many matrix elements are included as before. The anti-symmetric matrix is set up in a similar way. Its diagonal elements are $D_s - V_{ss'}$ and the off-diagonal elements are $V_{Is} - V_{Is'}$.

For each matrix the procedure of the one-state model is applied. This will give the evolution of a symmetrized initial mode $|I+\rangle$ and of an antisymmetrized mode $|I-\rangle$. The evolution of the local mode is just the average of these since the evolution equation is linear and, at $t = 0$,

$$|I\rangle = 1/\sqrt{2}|I+\rangle + 1/\sqrt{2}|I-\rangle. \tag{20}$$

When substituted into (18) this divides the coefficients by 2 and introduces cross terms into the beats. We note here that Stannard and Gelbart [3] take the initial state as $|I+\rangle$ so their solution is confined to the symmetrical modes.

The conclusion from this is that the system has a drop in amplitude of the initial mode from 1 to c_I, as given by (17), due to the transfer of energy to other modes induced by V.

4. The molecular potential for water and its spectrum

As has been shown earlier by Stannard et al. [6] the vibrations of water can be described to good accuracy using a potential based on local coordinates viz. the

Table 1. Morse parameters and vibrational energy constants of the local modes

	D_e (cm^{-1})	a	ω (cm^{-1})	ωx (cm^{-1})
Stretch	38838	2.34($Å^{-1}$)	3905	98
Bend	99822	0.42	1597	6
Stretch-stretch coupling −5084 ($cm^{-1}/Å^2$)				
Stretch-bend coupling 11 025 ($cm^{-1}/Å$)				

$r_e = 0.9572$ Å; $\theta = 104.52°$

stretch of the two OH bonds and the bend of the molecular angle at O. This potential is described here by Morse potentials in these local coordinates rather than by a Taylor expansion so that the anharmonicity can be already included in the local wavefunctions. The local modes are coupled by potential terms which are bilinear in the variables. The kinetic energy, because of the elimination of the centre of mass motion, has terms which also couple the three local coordinates bilinearly. By relating this Hamiltonian to the Taylor expansion, values of the Morse parameters can be derived which give a close fit to the Taylor parameters, derived from the experimental vibration spectra, as reported by Hoy et al. [7]. The values of the Morse and interaction parameters used are given in Table 1.

The spectrum was calculated for this Hamiltonian and compared directly to experiment. The states included in the calculation were those having up to 5 quanta in each local mode. The wavefunctions are products of three Morse wavefunctions and are, therefore, normal and orthogonal. They are denoted by *lmn*, where *l* is the number of quanta in the first OH stretch, *m* in the second and *n* in the bend. The accuracy with which this Hamiltonian and this finite basis can reproduce the experimental vibration spectrum is shown by the selected results in Table 2. The column headed "Exact" gives the frequencies calculated

Table 2. Vibrational energies (cm^{-1}) for H_2O

State	Expt.	Exact	When initial state is		
			100	002	221
(000)		(4649)			
(001)	1595	1577	1581	1584	1584
(002)	3152	3132	3146	3128	3156
(100)	3657	3669	3667	3669	3659
(010)	3756	3757	3753	3758	3758
(003)	4667	4676	4715	4715	4715
(101)	5235	5235	5243	5250	5243
(011)	5331	5333	5342	5342	5342
(004)	6136	6212	6261	6261	6261
(102)	6775	6799	6815	6815	6815
(012)	6872	6883	6914	6914	6914
(200)	7201	7198	7213	7213	7212
(020)	7250	7242	7228	7228	7228
(110)	7445	7455	7417	7417	7417

from the eigenvalues of the Hamiltonian. It is convenient to label the eigenstates as (*lmn*), where *lmn* is the mode which makes the largest contribution to the eigenfunction, except that (*lmn*), when $l > m$, now denotes the symmetric mode based equally on *lmn* and *mln* and, when $l < m$, their anti-symmetric mode. For frequencies less than 20 000 cm^{-1} the comparison with experiment is good to very good. For higher frequencies some differences become apparent but no drastic discrepancy is found. For the lower frequencies these local modes relate well to the eigenfunctions since, once the degeneracy of the two stretches is resolved by taking the sum and difference of *lmn* and *mln* modes, the result is a very close approximation to the eigenfunction. For the higher frequencies the states become closer in frequency and the local modes are mixed much more together in the normal modes. This result confirms the finding of Stannard and Gelbart [3] on the same molecule using a smaller set of local modes.

With this Hamiltonian the evolution of an initial state was calculated for a variety of choices of initial state. The exact solution was calculated using (5). The graphs of $P(t)$, the probability of finding the system in the initial state at a later time, were plotted and examined. Four examples, which indicate the variety of results obtained, are shown in Figs. 1-4. Some features are immediately apparent. The graph of 100 is dominated by the resonance of this initial mode with 010. This gives a beat between (100) and (010) with an amplitude of 0.488 which is almost the maximum possible amplitude. The graphs of 101, 102, and 103 are very similar but show a few ripples of high frequency. Fig. 2 for 002, in contrast, shows a large value of $\langle P \rangle$ and only a small amplitude of beat so P remains close to 1. This is caused by the large value of c_{II}, which is the coefficient of the initial mode in (3), the small amplitude of the beat between (002) and (100) and the very small amplitude of all other beats. Again, 001 and 003 are very similar graphs. Neither of these figures shows the initial dephasing drop which is expected. This is a little more evident in Fig. 3 for 221. The graph for 303 in Fig. 4 shows a more pronounced drop.

To understand these and other features of the results the one-state model was used. This makes it much easier to identify and label the beats. As is already

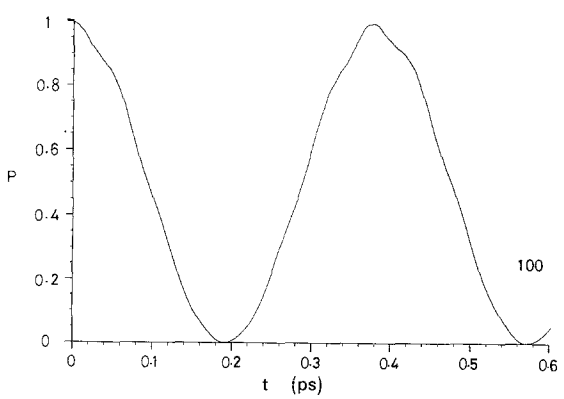

Fig. 1. The probability of finding the 100 vibrational mode excited at a later time. t is in picoseconds

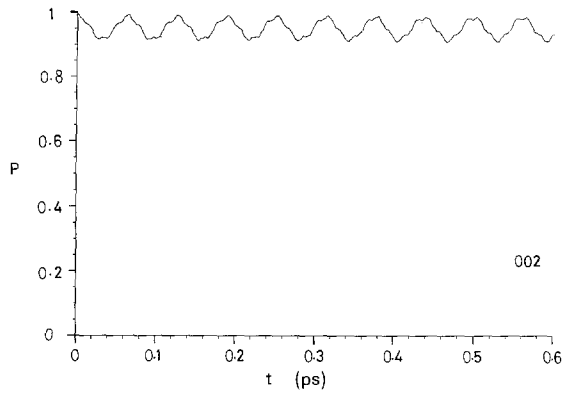

Fig. 2. The probability of finding the 002 vibrational mode excited at time t

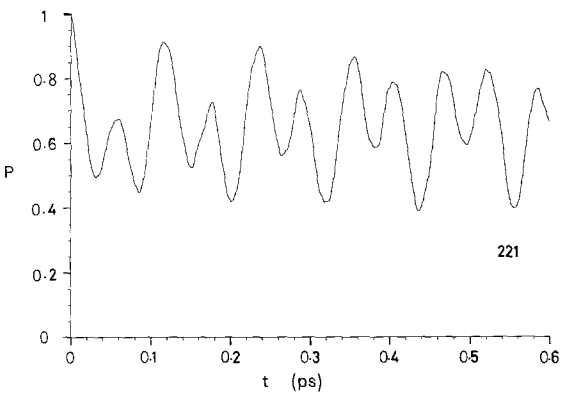

Fig. 3. The probability of finding the 221 vibrational mode excited at time t

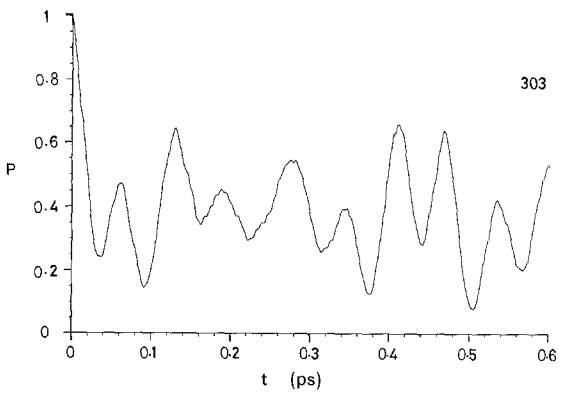

Fig. 4. The probability of finding the 303 vibrational mode excited at time t

apparent from Figs. 1 and 2, it is essential to distinguish sharply between the degenerate and non-degenerate initial states since their behaviour contrasts markedly and this model does so.

5. Degenerate initial states

When the initial state is degenerate, i.e. of the form *lmn* with $l > m$, the evolution is dominated by this degeneracy. The *lmn* and *mln* modes have the same energy before the coupling is included. They then split into symmetric and antisymmetric modes with slightly different energies. The probability oscillates between these with a low frequency and this determines the profile of the curves. On this are superimposed ripples due to other modes interacting with both states. The profile is determined by the l and m values and the ripples primarily by the value of n.

As the energy of the initial mode increases these evolutions show more and more a fast initial drop in probability which is never recovered. The origin of this effect is the coupling of these modes to those of much higher energy. This results in vibrations too rapid to show up on the scale of the graph. When there are several of these modes with similar amplitudes then, after a few periods, their phases, which were originally identical, will become unrelated so they will interfere destructively and average out to a zero displacement. The beginning of this effect is already visible in some of these curves. The 221 graph, for example, shows a vibration with declining amplitude caused by two interacting states of similar energy, (311) and (213). At $t = 0$ they are in phase but after a period they have lost this coherence and have begun to cancel. Unless their frequencies are in a rational relation they will never again be exactly in phase. Since the density of states increases with energy this kind of dephasing will occur more readily with the higher states.

6. Non-degenerate initial state

When the initial mode is non-degenerate, i.e. of the form *lln*, there are some common features in the results which we can analyse. In all of these, with the exception of 222, the probability shows a small amplitude of vibration and remains well above 0. The 00*n* graphs in particular, in which only the bending is excited, stay close to the value 1. This is a consequence of the relative purity of the initial local mode resulting in a large c_{II} and a large $\langle P \rangle$. It is helped by the fact that the vibration remains symmetric so that the anti-symmetric states are not excited. 222 is the only one which falls almost to 0 since the normal mode (222) is more of a mixture, mainly with the symmetric (320) state, which is almost degenerate with it. Generally, as n increases, the graphs become less smooth and higher frequency components are visible. There is little sign of an initial de-phasing drop in most of these results though, for 112 which has very near degeneracies with both (202) and (210), a drop is found.

7. The initial drop

To understand the results in a more quantitative way we have applied the one-state model. The symmetric and anti-symmetric modes are treated separately. Using these equations we have predicted values of the beat amplitudes and frequencies for each choice of initial state. The columns in Table 2 show the accuracy of this approximation to the frequencies under three of the modes illustrated earlier. From this calculation the identity of each beat can be decided and its amplitude found.

The beats cause P to vary around its average value $\langle P \rangle$. However, some of this variation is persistent while the rest is not. We suggest the hypothesis that the first part is that due to one dominant interaction, i.e. the beat with largest amplitude. In most of the examples this amplitude is considerably larger than those of the others and its frequency is lower so it appears to act as a signal in the presence of noise. This argument is supported by the realization that, if there were only one interaction, P would be a simple vibration with constant amplitude around $\langle P \rangle$ whereas two or more interacting modes with similar amplitudes and no common period are a model for random noise. From this hypothesis the drop in P is defined by

$$d = 1 - \langle P \rangle - 2c_l c_m, \tag{21}$$

where c_m is the largest coefficient, other than c_l, in (19). This equation enables the drop due to dephasing to be predicted easily for all the states. For some large drops the one-state model was not accurate enough and the numerical solution was used instead.

This drop can also be estimated by direct examination of the graphs. Some graphs have a clear indication of a drop but in others the estimate of the size of the drop is more subjective. A crude measure of drop is the difference between the initial value of 1 and the largest subsequent maximum. The major limitation of this definition is the finite size of the time interval T over which P is plotted. The values of the drop according to these two definitions were found and examples are shown in Table 3 for the modes of Figs. 1–4. More generally their relation is shown in Fig. 5. The drop calculated from (21) is almost always greater than the graphical estimate and this suggests that the maximum beat may not be the only persistent part of the probability or that the graphical maximum may contain a ripple which hides part of the drop or that the one-state estimates may be too

Table 3. Drop in probability due to dephasing

Mode	Graph estimate	Calculated from (21)	c_l
100	0.01	0.023	0.489
002	0.01	0.007	0.977
221	0.08	0.106	0.755
303	0.33	0.734	0.212

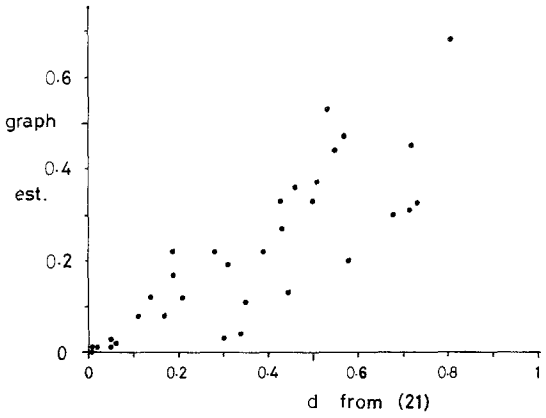

Fig. 5. The graphical estimate of the drop and the calculated d from Eq. (21)

high. However, the trends in the two measures are sufficiently in agreement to give justification to our definitions.

Figure 6 is a graph showing the calculated drop for many initial modes as a function of their (symmetrical) state energy. It shows how the size of this drop increases with energy in dramatic fashion in the range above 20 000 cm^{-1}. States with the same l and m show a gradual rise in drop with n. States with $n = 0$ are generally low and those with $m = 0$ are generally high. States with the same value of $l + m$ and n have a similar energy and their drop increases as m decreases.

8. Propensity rules

It is of considerable interest to formulate rules which indicate the selection of those modes which interact most strongly with any given initial state. Because we have an exact calculation we can discover the origin of these rules more easily than from an analysis of experimental results.

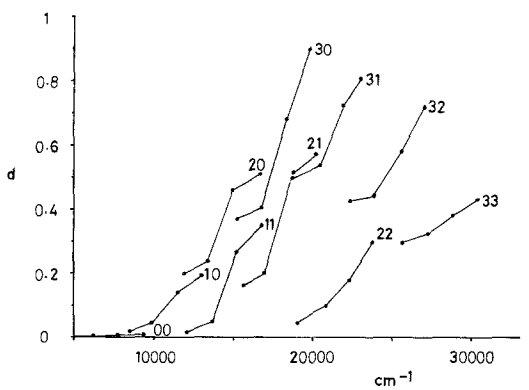

Fig. 6. The drop d as a function of energy of the initial state lmn. Lines connect states with the same lm. $n = 3$ for the state most to the right and decreases to the left along the line

Table 4. Initial modes and their interacting states

Mode	Interacts with	Beat amp.	Beat freq. (cm^{-1})
100	(001)	0.49	87
200	(020)	0.40	55
	(110)	0.06	269
110	(200)	0.22	282
310	(130)	0.23	131
	(122)	0.08	63
	(220)	0.07	329
311	(131)	0.21	135
	(123)	0.08	122
	(221)	0.06	318
	(213)	0.04	275
323	(233)	0.06	156
	(241)	0.02	121
	(421)	0.02	4
333	(325)	0.18	671
	(431)	0.04	481

For this Hamiltonian there is one selection rule which plays a major part in the evolution. This is that modes must have exactly two different quantum numbers to have a non-zero interaction in V. This is a consequence of using only bilinear couplings in the kinetic and potential energy terms. There is also one selection rule for the eigenfunctions which is important. This is the symmetric/anti-symmetric rule which has already been emphasized. Degenerate modes have both symmetry types and mix with all states whereas the non-degenerate modes mix only with the symmetric states.

Apart from these rules the selection of mixing modes seems to be related to Fermi resonance. Thus 002 is close in energy to 100 and 010 and 110; 200, 020; 102 and 012 are even closer so these are the modes which mix. As the energy increases such near degeneracies become more numerous since more options are available, e.g. 400, 310, 220, 302, 212, 204, 114. The magnitude of the coupling interactions increases with the number of quanta in a mode especially when that number increases by one. Thus, for example 400 has matrix elements in descending order of magnitude with 501, 301, 502, 302, 310, 201. On the other hand it has a very small V element with 040 because the two modes have four quanta different; this gives a very small direct split between their symmetric and anti-symmetric combinations. The indirect split due to the coupling of each with other states is more substantial and is also the cause of the large drop. Table 4 shows, for a selection of initial modes the modes that interact most strongly, arranged in order. As Eq. (17) shows, this is related both to V and to the difference in eigenvalues.

9. Density of states

In the energy range considered these states are all discrete so, strictly speaking, there is no density of states. Nevertheless the idea is a useful one since it helps

to rationalize the results and makes it easier to connect with other statistical considerations. If the density is defined as N, the number of states within a band of width $\pm 500\ \mathrm{cm}^{-1}$, then a block diagram can be drawn covering the range of interest. This is shown in Fig. 7. It has maxima at energies corresponding to the near degeneracies noted above and with heights proportional to their number.

From Fig. 7 it can be seen that the density at low energies is very low and that it increases quickly around $20\,000\ \mathrm{cm}^{-1}$. The correlation with the trend in Fig. 6 seems to indicate that the number of Fermi resonances is important for the drop. On the other hand Fig. 7 also shows that modes with almost the same energy, and so the same density, can have very different drops. This emphasizes the fact that the drop also depends on the magnitude of the matrix elements of V.

In some discussions of dephasing, e.g. [5], the discussion uses the golden rule which gives an interaction proportional to the density of states and a P which decreases linearly or exponentially with time. In this treatment the initial decrease is always quadratic but inspection of some graphs suggests that, when the drop is considerable, it often approximates to a linear descent. Presumably this is due to the superposition of many quadratic drops. The golden rule itself cannot be the only factor since we have shown conclusively that symmetry plays a dominant role in all aspects of the results. Furthermore the profile of the beat amplitudes is not usually of Lorentz form. On the other hand the amplitude does have a form which resembles this in some circumstances. If one interacting mode m has a much larger matrix element V_{Im} than the others the initial amplitude using (17) becomes

$$c_I = 1/(1 + V_{Im}V_{mI}/(z_I - D_m)^2) = (z_I - D_m)^2/((z_I - D_m)^2 + V_{Im}V_{mI}), \qquad (22)$$

which is Lorentz like with the product $V_{Im}V_{mI}$ acting as the damping factor despite the fact that the beat is not damped.

The value of c_I depends on two factors. One is the matrix element V_{Is} and because of the bilinear form of the Hamiltonian many near degenerate modes have a zero or very small element. The $1/(z_I - D_s)$ factor is an inverse energy spacing and so can be considered as the origin of the density of states dependence in c_I. Practical calculations show that c_I can be found, to reasonable accuracy, using

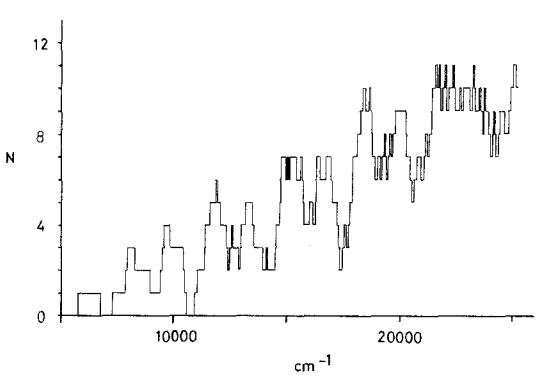

Fig. 7. Density of states. N is the number of states within $\pm 500\ \mathrm{cm}^{-1}$

only 3 or 4 of the nearest interacting states. Since a non-zero V_{Is} has a magnitude in the range 100–300 cm^{-1}, states within a range of $\pm 500\ cm^{-1}$ make the major contribution. Thus the determining factor is not just the density of states but the density of *interacting* states. This helps us to understand why near degenerate states, with the same density of states, can have very different values of c_I.

10. Role of the amplitude of the initial mode

As a means of organizing the observations we have found that the amplitude of the initial mode c_I is a useful and appropriate variable. For the non-degenerate modes this is always the largest amplitude. Since the amplitudes are positive and sum to unity the size of c_I limits the size of all other amplitudes. From the definition it is clear that the drop is limited by

$$d < 1 - c_I^2 \tag{23}$$

but this is not a very tight bound.

A more interesting relation is found by adopting the simple hypothesis that other amplitudes in turn will each take half the remaining amplitude. This puts them into a geometric sequence which is easy to manipulate. For some initial states it represents a fair approximation but for others it serves only as a crude estimate of a complicated situation. From this the drop is estimated to be

$$d = 2/3 - c_I/3 - c_I^2/3. \tag{24}$$

Fig. 8 shows this relation along with the calculated drops for some non-degenerate modes as a function of c_I. It can be seen that the relation is not close but it does thread through the points. Apart from a few points the calculated drops seem to follow another curve whose origin we have not discovered.

For the degenerate modes the corresponding argument is more useful. The symmetric and antisymmetric amplitudes separately add to 1/2. For each symmetry the state derived from the initial mode and its partner will usually be the largest amplitudes. For some higher energy states this is not true and these fall outside these considerations. Often these two are very comparable in size though the antisymmetric one is usually a little larger since it has fewer modes to interact with it and reduce its size. If these are taken as equal then the inequality corresponding to (23) is

$$d < 1 - 4c_I^2. \tag{25}$$

However, the assumption of geometric amplitudes leads to the relation

$$d = 5/6 + 2c_I/3 - 14c_I^2/3. \tag{26}$$

Figure 9 shows this relation along with the points for some of these degenerate initial modes. The results are closer to the curves and show how the constraints due to symmetry serve to limit the possible values.

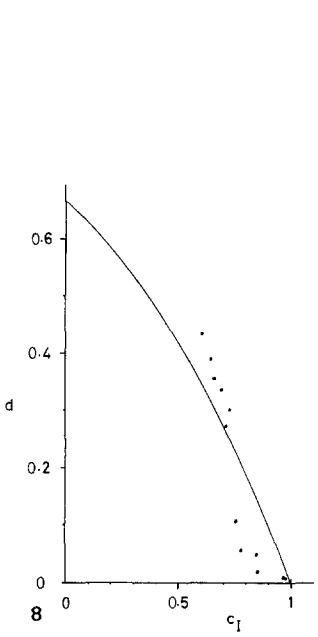

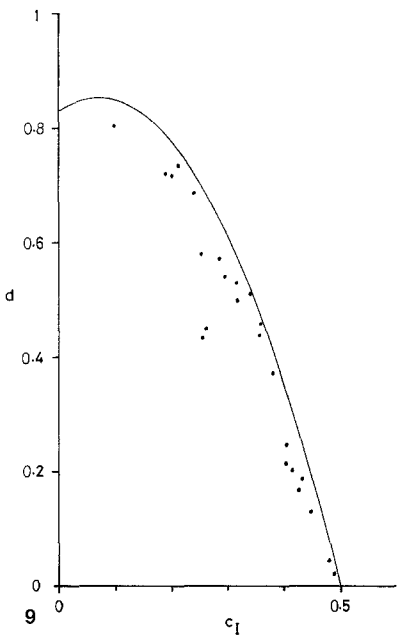

Fig. 8. Calculated drop as a function of the initial state coefficient c_I for non-degenerate modes. Curve is given by Eq. (24)

Fig. 9. Calculated drop as a function of the initial state coefficient c_I for degenerate modes. Curve is given by Eq. (26)

The dominant influence of c_I on the results is apparent from these figures even though we have not been able to derive a precise equation for the relationship.

11. Conclusions

We have shown that the evolution of a vibrationally-excited water molecule is governed by several considerations. Symmetry plays an important role and divides the results into categories depending on the degeneracy or not of the initial mode. At low energies the degenerate modes have quantum beats with large amplitudes whereas the non-degenerate modes do not. At higher energies a dephasing drop is observed due to the stronger coupling of the local mode to the high frequency modes. This is more apparent in degenerate modes since these interact with both symmetric and anti-symmetric states whereas the non-degenerate modes involve only the symmetric states. The dephasing drop has been analysed and a formula for its calculation given and partly justified. Some propensity rules for the selection of important interacting states have been suggested. The role of the amplitude of the initial state in determining the drop has been illustrated.

Although the water molecule has some idiosyncratic features, such as the pattern of its near resonances, the general principles that have emerged in this study should apply to many other small molecules.

The possibility of experimental observation of the phenomena considered here has not been discussed. Since the direct excitation of a single local mode is difficult to achieve it cannot be easy. Indirect excitation of non-stationary vibrations through molecular fluorescence is possible but the resulting dephasing is too rapid for most experiments to measure. The observational conditions necessary to observe intramolecular energy transfer and quantum beats have been fully discussed by Freed and Nitzan [2].

Acknowledgement. The authors wish to acknowledge their thanks to the Data Processing Center, Kyoto University, for the use of the computer.

References

1. Weitz E, Flynn G (1981) Adv Chem Phys 43:185
2. Freed KF, Nitzan A (1980) J Chem Phys 73:4765
3. Stannard PR, Gelbart WM (1981) J Phys Chem 85:3592
4. Ivanco M, Hager J, Sharfin W, Wallace SC (1983) J Chem Phys 78:6531
5. Ramaswamy R, Augustin S, Rabitz H (1978) J Chem Phys 69:5509
6. Stannard PR, Elert ML, Gelbart WM (1981) J Chem Phys 74:6050
7. Hoy AR, Mills IM, Strey G (1972) Mol Phys 24:1265